

Communication-free Cohesive Flexible-Object Transport using Decentralized Robot Networks

Yoshua Gombo, Anuj Tiwari and Santosh Devasia

Abstract—Decentralized network theories focus on achieving consensus and in speeding up the rate of convergence to consensus. However, network cohesion (i.e., maintaining consensus) during transitions between consensus values is also important when transporting flexible structures. Deviations in the robot positions due to loss of cohesion when moving flexible structures from one position to another, such as uncured-composite aircraft wings, can cause large deformations, which in turn, can result in potential damage. The major contribution of this work is to develop a decentralized approach to transport flexible objects in a cohesive manner using local force measurements, without the need for additional communication between the robots. Additionally, stability conditions are developed for discrete-time implementation of the proposed cohesive-transition approach, and experimental results are presented, which show that the proposed cohesive transportation approach can reduce the relative deformations by 85% when compared to the case without it.

I. INTRODUCTION

The main goal is to transport flexible objects cohesively (i.e., all robots move in a similar manner) using decentralized robot networks. Network control theories can be used to rapidly transition from one equilibrium (where all the robots in the network are in consensus) to another, i.e., a new consensus value, which also can be applied for transporting an object using robot networks. However, current network theories focus on the speed of convergence to a new consensus value [1], [2], and they do not aim to ensure that the robot responses remain cohesive during transition. For a transport task, the lack of cohesion during transition can lead to large deformation and cause damage to the object being transported. While centralized communication can yield to low-deformation transport [3], [4], there is a growing interest in decentralized transport using a robot network that only uses local sensing due to robustness to one or more robot failures [5], [6], adaptability to varying number of robots [7], [8], and versatility to transport different objects [5], [9], without the need for centralized control and communication [10]. The main contributions of this paper are to propose a cohesive transport approach for flexible structures with decentralized robot networks, and to establish stability conditions for a discrete-time implementation using local force sensing.

Observation in nature indicates that ants seem to use local force measurement in their movement to transport foods, rather than communicating explicitly, e.g., [11]. Similarly, in a transport task the elasticity of the object can be used

to transmit information (i.e., forces and positions) among neighbors in network, instead of communicating with each other. For example, as shown in [7], [12]–[14] measurements of the local force exerted between the flexible object and robot can be used to infer the local deformation and accomplish the transport task in a decentralized manner. Alternatively, changes in the desired shape of the object can also be measured to develop a decentralized feedback control for object transport, e.g., [15]–[17]. While such methods can be used to achieve transport of flexible objects from one position to another, say within some specified settling time, there is no direct control over the resulting deformations on the object. In the presence of only a few leaders (who have access to desired transport trajectory), there can be substantial deviation in the robot positions away from the leaders resulting in distortion and potential damage. For example when transporting uncured-composite aircraft wings, large deformations can lead to structural damage. If all the robots are leaders with access to the desired transport trajectory, then the network response would be cohesive, but this leads to a centralized approach, and such communication might not be always feasible, e.g., if one of the robots is directly controlled by a human and the others follow based on neighbor-based observations or local sensing of the object. This motivates the current effort to improve cohesion during decentralized transport of flexible objects.

This work aims to reduce deformations of the object being transported by developing methods for cohesive positioning of the robot network. Recent studies have shown that control laws can be developed to improve cohesion of decentralized networks using Delayed Self Reinforcement (DSR) [18]. The main contribution of the current paper is to develop an approach to transport objects using the cohesive method in [18], without the need for inter-robot communications - rather, only the local force measurements are required. Specifically, the current work (i) shows that the DSR approach can be used to achieve cohesive transport using only local force measurements, without the need of inter-robot communication, and (ii) establishes stability conditions for the discrete-time implementation of the proposed cohesive transport approach. Furthermore, experimental results are used to show that the proposed approach improves network cohesion, and leads to low-deformation transport of flexible objects.

II. PROBLEM FORMULATION

In this section, the deformation control issue with local force-based decentralized transport dynamics is presented along a single axis- y . Similar approaches can be used for the other axes of motion.

A. Local-force feedback as a network-based update

The robots are attached to a flexible object, e.g., as shown in Fig. 1. The position $y_k \in \mathbb{R}$ of each robot k in the network is updated using local force measurements $f_k \in \mathbb{R}$ as well as a virtual force $\tilde{f}_k = \hat{k}_{k,d}(y_k - y_d) \in \mathbb{R}$ if robot k is a leader, as

$$y_k[m+1] = y_k[m] - \gamma \hat{f}_k[m], \quad (1)$$

$$\hat{f}_k[m] = f_k[m] + \tilde{f}_k[m], \quad (2)$$

where the update sampling-time period is δ_t , $y_k[m]$ represents the position of robot k at discrete time instants, e.g., $y_k[m] = y_k(m\delta_t)$, γ is the update gain, and the desired position from the virtual source $y_d \in \mathbb{R}$ is known (i.e., $\hat{k}_{k,d} \neq 0$) only if robot k is a leader, e.g., $k=1$ in the example in Fig. 1. Each robot position y_k is measured from an initial undeformed configuration (with all $y_k = 0$) of the flexible object.

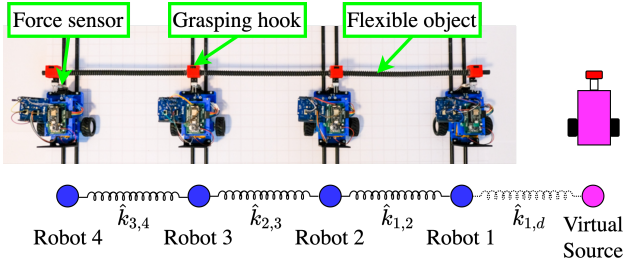


Fig. 1: Top: Experimental setup of flexible load transport. Bottom: Schematic network model where the leader, robot $k=1$, aims to match the position of the virtual source (pink).

The local force-based robot position update in Eq. (1) achieves object transport, i.e., for a fixed desired position y_d , the network reaches equilibrium when each robot reaches the desired position, i.e., $y_k = y_d$ for all k and the object has no distortion, i.e., $f_k = 0$. To clarify, note that the local force f_k measured by robot k can be written linearly in terms of the position y_j of all robots connected to robot k , provided the local deformation of the flexible object remains small, as

$$f_k[m] = \sum_{j=1}^n \hat{k}_{k,j}(y_k[m] - y_j[m]), \quad (3)$$

where $\hat{k}_{k,j} = \hat{k}_{j,k} \geq 0$ is the effective stiffness of the flexible object between two neighboring robots j and k , n is the number of robots, and $\hat{k}_{j,j} = 0$ for all $1 \leq j \leq n$. Then, the update law in Eq. (1) can be written in matrix form as

$$\mathbf{Y}[m+1] = (\mathbf{I} - \gamma \mathbf{K})\mathbf{Y}[m] + \gamma \mathbf{B}y_d[m], \quad (4)$$

where $\mathbf{Y} = [y_1, y_2, \dots, y_k, \dots, y_n]^T \in \mathbb{R}^n$ is the n dimensional vector of the individual robots positions y_k , $B_k = \hat{k}_{k,d}$ is the k^{th} element of n dimensional vector $\mathbf{B} \in \mathbb{R}^n$ which is nonzero

only if the robot k is a leader and the symmetric matrix \mathbf{K} is the pinned Laplacian with elements

$$\begin{aligned} \mathbf{K}_{k,j} &= \hat{k}_{k,d} + \sum_{m=1}^n \hat{k}_{k,m} \geq 0 & \text{if } k=j \\ &= -\hat{k}_{k,j} & \text{otherwise,} \end{aligned} \quad (5)$$

with real nonzero eigenvalues $\lambda_{\mathbf{K},j} > 0$ for $1 \leq j \leq n$. It can be shown that for an update gain γ satisfying

$$0 < \gamma < \left(\bar{\gamma} = 2/\bar{\lambda}_{\mathbf{K}} = 2/\max_j(\lambda_{\mathbf{K},j}) \right), \quad (6)$$

the eigenvalues of $(\mathbf{I} - \gamma \mathbf{K})$ are inside the unit circle. Therefore, the transport dynamics in Eq. (4) is stable, and the desired transport of the object can be achieved, i.e., for a fixed desired position y_d , the robot positions in \mathbf{Y} converge to the desired value [19]

$$\lim_{m \rightarrow \infty} \mathbf{Y}[m] = \mathbf{1}_n y_d \quad (7)$$

with $\mathbf{1}_n$ representing the n dimensional vector of all ones.

B. Problem: improve cohesion for similar settling time

The settling time T_s to a new desired position y_d can be selected by choosing the update gain γ . In particular, the settling time T_s to reach and stay within 2% of a step change in the desired displacement y_d can be estimated as

$$T_s \approx \frac{-4 \delta_t}{\ln(\lambda_{\mathbf{K}}^*)} \quad \text{where } \lambda_{\mathbf{K}}^* = \arg \max_{\lambda_{\mathbf{K},j}} |1 - \gamma \lambda_{\mathbf{K},j}|. \quad (8)$$

However, for a given settling time (i.e., given selection of the update gain γ), the deformations during transport can not be controlled further. Typically, faster settling (i.e., a smaller settling time T_s) also results in larger deformation. The research problem addressed here is to improve cohesion, i.e., to reduce the maximum deformation \bar{D} of the object during transport,

$$\bar{D} = \max_m \left[D[m] = \max_{k,j} |(y_j[m] - y_k[m])| \right], \quad (9)$$

without increasing the settling time T_s .

III. TRANSPORT USING COHESIVE DSR

A. Cohesive transport using local force measurements

The robot-position update to transport the object is chosen as a discrete-time approximation of an ideal cohesive network. For example, in the continuous time case, if each robot had access to the desired position y_d , i.e., in a centralized approach, then the ideal cohesive update can be written as,

$$\dot{\mathbf{Y}}(t) = -\alpha \mathbf{Y}(t) + \alpha \mathbf{1}_n y_d(t), \quad (10)$$

where the gain $\alpha > 0$ can be tuned to achieve a desired settling time and all robot move in a similar manner. The lack of access to centralized information about the desired position y_d can be alleviated by multiplying both sides with the scaled pinned Laplacian $\beta \mathbf{K}$, substituting $\mathbf{K} \mathbf{1}_n$ with \mathbf{B}

[18], and adding $\dot{\mathbf{Y}}$ to both sides and rearranging the equation to obtain

$$\begin{aligned}\dot{\mathbf{Y}}(t) &= -\alpha\beta\mathbf{K}\mathbf{Y}(t) + \alpha\beta\mathbf{B}y_d(t) + [\mathbf{I} - \beta\mathbf{K}]\dot{\mathbf{Y}}(t), \\ &\approx -\alpha\beta\mathbf{K}\mathbf{Y}(t) + \alpha\beta\mathbf{B}y_d(t) + [\mathbf{I} - \beta\mathbf{K}]\frac{\mathbf{Y}(t) - \mathbf{Y}(t - \tau)}{\tau}.\end{aligned}\quad (11)$$

$$(12)$$

With the time delay $\tau = \delta_t$ and the update kept constant between sampling periods, the update law in Eq. (12) for robot positions becomes

$$\begin{aligned}\mathbf{Y}[m+1] &= \mathbf{Y}[m] - \alpha\beta\delta_t\mathbf{K}\mathbf{Y}[m] + \alpha\beta\delta_t\mathbf{B}y_d[m] \\ &\quad + [\mathbf{I} - \beta\mathbf{K}](\mathbf{Y}[m] - \mathbf{Y}[m-1]).\end{aligned}\quad (13)$$

Then for each robot k , the update law becomes

$$\begin{aligned}y_k[m+1] &= y_k[m] - \alpha\beta\delta_t f_k[m] + \alpha\beta\delta_t \hat{k}_{k,d}(y_d[m] - y_k[m]) \\ &\quad + (1 - \beta\hat{k}_{k,d})(y_k[m] - y_k[m-1]) \\ &\quad - \beta(f_k[m] - f_k[m-1]).\end{aligned}\quad (14)$$

Note that this cohesive transport law is decentralized. For each robot, in addition to the virtual source position y_d if the robot is a leader, the update only requires current information and delayed self reinforcement (DSR) by a time step of: (i) local force measurements f_k and (ii) its own position y_k .

B. Stability of cohesive DSR

Stability conditions can be established by finding the roots of the characteristic equation of the cohesive dynamics in Eq. (13), i.e.,

$$\det(\mathbf{I}z^2 - (\mathbf{I} - \alpha\beta\delta_t\mathbf{K}_J + [\mathbf{I} - \beta\mathbf{K}_J])z + [\mathbf{I} - \beta\mathbf{K}_J]) = 0, \quad (15)$$

where $\mathbf{K}_J = \mathbf{P}_\mathbf{K}^{-1}\mathbf{K}\mathbf{P}_\mathbf{K}$ is the diagonalization of the pinned Laplacian \mathbf{K} with eigenvalues $\lambda_{\mathbf{K},k}$ along the diagonal. In particular, the cohesive dynamics in Eq. (13) is stable if and only if, for each eigenvalue $\lambda_{\mathbf{K},k}$ of the pinned Laplacian \mathbf{K} , the roots of $D(z)$ where

$$\begin{aligned}D(z) &= z^2 - (1 - \alpha\beta\delta_t\lambda_{\mathbf{K},k} + [1 - \beta\lambda_{\mathbf{K},k}])z \\ &\quad + [1 - \beta\lambda_{\mathbf{K},k}] = 0\end{aligned}\quad (16)$$

have magnitude less than one. Thus, stability can be evaluated by computing the roots of Eq. (16). Nevertheless, for design purposes, it is preferable to establish analytical conditions on the DSR parameters for stability, as shown next.

Lemma 1: The proposed cohesive DSR based dynamics in Eq. (13) is stable if and only if the gains α, β satisfy the following conditions for the largest eigenvalue $\lambda_\mathbf{K}$ of the pinned Laplacian \mathbf{K} :

$$\begin{aligned}(i) \quad &0 < \alpha \\ (ii) \quad &0 < \beta < \frac{4}{\lambda_\mathbf{K}(\alpha\delta_t + 2)}.\end{aligned}\quad (17)$$

Proof: Proof of Lemma 1 follows from Jury stability test and is omitted here for brevity.

Remark 1: The delay in Eq. (12) can be defined over multiple samples, i.e., $\tau = N\delta_t$ where $N \geq 1$ is an integer number. However a larger delay τ (larger N) reduces the effectiveness of the approximate derivative in Eq. (12) and thereby, reduces the ability to track faster signals in a cohesive manner [18].

IV. EXPERIMENT AND PARAMETER SELECTION

A. System description

To easily visualize the deformation during transport, a highly flexible object (a long spring coiled with diameter of 1.30 cm and length of 90 cm) was selected for transport using a robot network as shown in Fig. 1. Only the leader (robot 1) has knowledge of the desired position illustrated by the virtual source shown in pink in Fig. 1. Each robot k measures the local force f_k using a force sensor between the robot and the object, and senses its position y_k using magnetic encoders on the wheels, and uses an on-board micro-controller to compute the next position $y_k[m+1]$. The updated position $y_k[m+1]$ is achieved within the sampling-time period $\delta_t = 0.03$ s, using a velocity feedback control to maintain the velocity at $v_{d,k}(t) = (y_k[m+1] - y_k[m])/\delta_t$ as shown in Fig. 2.

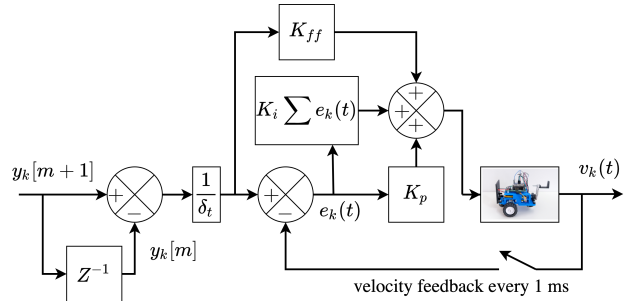


Fig. 2: Velocity-based feedback control system of robot k to achieve the position $y_k[m+1]$ using a proportional (gain K_p) and integral (gain K_i) feedback controller along with feedforward control (gain K_{ff}).

The system dynamics in Eq. (1) was found by estimating the elastic object stiffness $\hat{k}_{i,j}$ experimentally. In particular, for estimating $\hat{k}_{1,2}$, robot 1 was moved for a known distance y_1 without moving the other robots (nor connecting robot 1 to the virtual source) and the resulting force f_1 was measured to yield $\hat{k}_{1,2} = f_1/y_1$. Then, to estimate stiffness $\hat{k}_{2,3}$, robot 2 was moved for a known distance y_2 without moving the other robots and the resulting force f_2 was measured to yield $\hat{k}_{2,3} = (f_2/y_2) - \hat{k}_{1,2}$. The same procedure is used to obtain the rest of the effective stiffness coefficients, which are all the same and given by $\hat{k}_{i,i+1} = 0.05$ N/cm, for $1 \leq i \leq 3$, which is to be expected since the connecting springs have similar lengths. For the setup shown in Fig. 1, the stiffness of the connection with virtual source is chosen to be same as the other spring elements, i.e., $\hat{k}_{1,d} = 0.05$. The resulting

pinned Laplacian \mathbf{K} and matrix \mathbf{B} were

$$\mathbf{K} = \begin{bmatrix} \hat{k}_{1,2} + \hat{k}_{1,d} & -\hat{k}_{1,2} & 0 & 0 \\ -\hat{k}_{1,2} & \hat{k}_{1,2} + \hat{k}_{2,3} & -\hat{k}_{2,3} & 0 \\ 0 & -\hat{k}_{2,3} & \hat{k}_{2,3} + \hat{k}_{3,4} & -\hat{k}_{3,4} \\ 0 & 0 & -\hat{k}_{3,4} & \hat{k}_{3,4} \end{bmatrix}$$

$$= \begin{bmatrix} 0.10 & -0.05 & 0 & 0 \\ -0.05 & 0.10 & -0.05 & 0 \\ 0 & -0.05 & 0.10 & 0.05 \\ 0 & 0 & -0.05 & 0.05 \end{bmatrix}, \quad (18)$$

$$\mathbf{B} = [\hat{k}_{1,d} \ 0 \ 0 \ 0]^T = [0.05 \ 0 \ 0 \ 0]^T. \quad (19)$$

B. Selection of control parameters

To avoid optimization over each desired trajectory y_d , the control parameters are selected to minimize the deformation for a specified settling time T_s for a unit step change in the desired position y_d .

1) *Case without DSR*: The update gain γ is found numerically for a specified network settling time T_s when the position changes by a unit step. For update gains γ satisfying the stability condition in Eq. (6), the settling times T_s were estimated using Eq. (8), and are shown in Fig. 3a. Interpolation of this data can be used to find the update gain γ for a specified settling time T_s . In the following, the settling time $T_s = 10$ s is chosen in order to bound the maximum speed input to the robot $v_{d,k} = v_{nodsr}$ below the acceptable speed limit $v_{max} = 5$ cm/s as shown in Fig. 4b. The corresponding update gain $\gamma = 1.93$ and the step response is shown in Fig. 4a.

2) *Case with cohesive DSR*: To enable comparative evaluation, the cohesive DSR parameters (α, β) are selected to match the settling time T_s of the case without DSR, and the maximum speed input $v_{d,k}$ is below v_{nodsr} for the case without DSR. Since it is possible to obtain multiple combinations of the parameters (α, β) that satisfy the settling time T_s and the maximum speed input $v_{d,k}$ conditions, the optimal parameters are selected such that the spectral radius σ is minimized (to maximize structural robustness), i.e.,

$$\sigma^* = \min_{\alpha, \beta} \left(\sigma(\alpha, \beta) = \max_j |z_j| \right), \quad (20)$$

subject to $v_{d,k} \leq v_{nodsr}$

where z_j is the j^{th} root of the characteristic equation $D(z)$ as in Eq. (16). The parameters (α, β) for the same range of settling time T_s as in the case without DSR are shown in Fig. 3b. In the following, the settling time $T_s = 10$ s is chosen to match the case without DSR and the corresponding parameters are

$$\alpha = 0.39 \approx 0.4, \quad \beta = 10.92 \approx 10.9. \quad (21)$$

The step response is also shown in Fig. 4a. Note that the maximum speed input to the robot $v_{d,k}$ is also well below v_{nodsr} as shown in Fig. 4b.

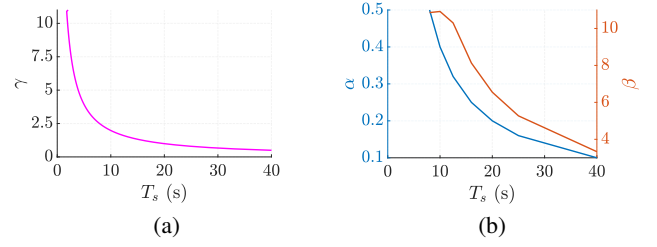


Fig. 3: Selection of control parameters with respect to settling time T_s : (left) The update gain γ for the case without DSR, (right) DSR parameters α and β for the case with cohesive DSR.

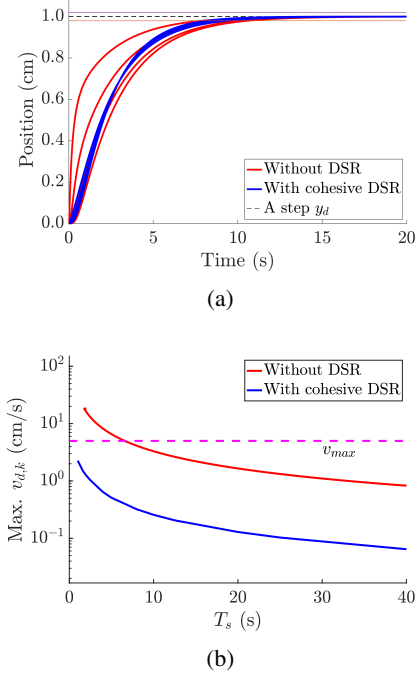


Fig. 4: (a) **Increase in cohesion with DSR**. Position responses for a step change in position y_d for both (i) without DSR ($\gamma = 1.93$) as in Eq. (4) and (ii) with cohesive DSR ($\alpha = 0.39, \beta = 10.92$) as in Eq. (13) which show that both settle within $T_s = 10$ s. (b) **Reduction of maximum input speed with DSR for the same settling time**. Selection of settling time T_s such that the maximum speed $v_{d,k}$ of the robot is below the acceptable speed limit v_{max} .

Remark 2: When the sampling time δ_t becomes small as compared to the transport time, the discrete time cohesive dynamics in Eq. (13) should be similar to the continuous-time ideal cohesive dynamics in Eq. (10). Therefore, the settling time becomes $T_s = 4/\alpha$ and can be selected using the parameter α . With the settling time chosen as $T_s = 10$ s, the estimate of $\alpha = 4/T_s = 0.4$ is close to the result from the numerical search $\alpha = 0.39$ in Eq. (21).

Remark 3: The spectral radius, provided the associated second-order dynamics in Eq. (16) is not overdamped, is the maximum value of $|1 - \beta \lambda_{\mathbf{K},k}|$, which is minimized over all eigenvalues $\lambda_{\mathbf{K},k}$, by selecting $\beta = \frac{2}{\lambda_{\mathbf{K}} + \bar{\lambda}_{\mathbf{K}}} = \frac{2}{0.006 + 0.176} = 10.95$, which is close to the result from the numerical search, $\beta = 10.92$ in Eq. (21).

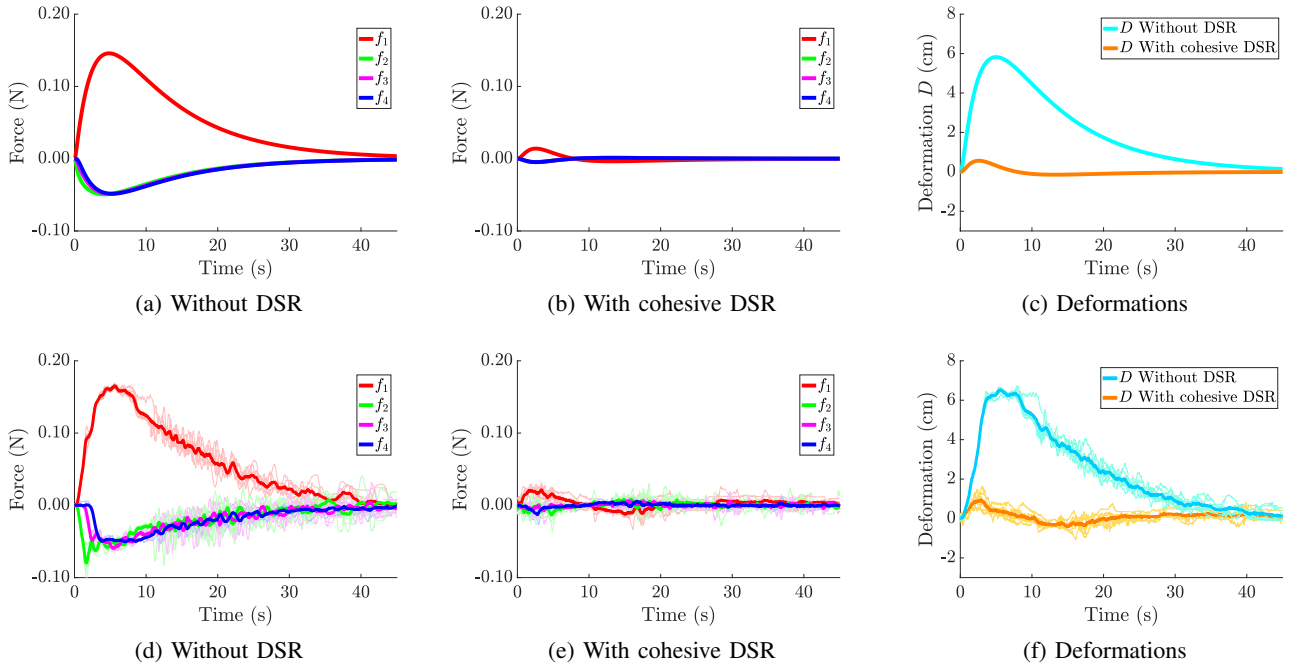


Fig. 5: Comparative evaluation of force f_k as in Eq. (3) and deformation D as in Eq. (9) with and without cohesive DSR, and similarity of simulations (top row) and experimental results (bottom row). Experiment results are shown for 7 trials (shown in thin lines), and the means are shown in thick lines.

V. RESULTS

A. Selection of the desired transport trajectory

A large change in position y_d from 0 cm to 50 cm was chosen to help visualize the transport of the flexible body. To ensure that the deformations are not too large (i.e., to avoid other robots dragging each other), the desired transport trajectory y_d was chosen as a step that is filtered using a first-order, low-pass filter with cutoff frequency ω_c and implemented using Tustin's approximation, as

$$y_d[m] = \frac{2 - \omega_c \delta_t}{2 + \omega_c \delta_t} y_d[m-1] + \frac{\omega_c \delta_t}{2 + \omega_c \delta_t} (y_{ds}[m] + y_{ds}[m-1]), \quad (22)$$

where $y_{ds}[m] = 50$ if $m > 0$ and zero otherwise. The effect of the cutoff frequency ω_c on maximum deformation \bar{D} in Eq. (9) is shown in Fig. 6a. The cutoff frequency ω_c was selected as $\omega_c = 0.1 \text{ rad/s}$ so that the maximum deformation \bar{D} is below 7 cm and the maximum speed input to the robot $v_{d,k} \leq (v_{max} = 5 \text{ cm/s})$ to avoid dragging of the robots by each other for the case without DSR. Note that the desired trajectory y_d reaches the final value of 50 cm in about $T_{sf} = 4/\omega_c = 40 \text{ s}$ as seen in Fig. 6b.

B. Results and discussion

Comparative evaluations, with and without the DSR approach, are presented below. The results are evaluated based on the maximum deformation \bar{D} in Eq. (9) and also the maximum force \bar{f} defined as

$$\bar{f} = \max_{k=\{1,2,3,4\}} \left(\max_m |f_k[m]| \right). \quad (23)$$

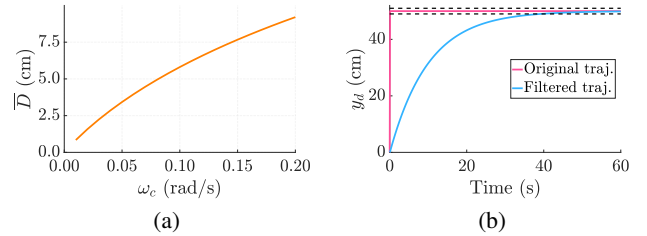


Fig. 6: (a) The effect of cutoff frequency ω_c on maximum deformation \bar{D} . (b) The desired trajectory y_d obtained by passing a step trajectory y_{ds} through a first-order, low-pass filter with cutoff frequency $\omega_c = 0.1 \text{ rad/s}$ as in Eq. (22).

The simulation and experimental results are shown in Fig. 5, and quantified in Table I. The responses from the experiments and simulations are similar to each other in Fig. 5, which indicates that the models are close to the experimental system. The cohesive DSR approach reduces the maximum deformation \bar{D} substantially, by 90% in simulation and $85 \pm 0.05\%$ in experiment. Similarly, the corresponding maximum forces \bar{f} are also reduced significantly, by 90% in simulation and $87 \pm 0.50\%$ in experiment. The reduction in deformation indicates that the robot network responses are more cohesive during transport with the cohesive DSR approach. This increased cohesion can also be observed from snapshots of experiment in Fig. 7.

Label	Without DSR	Cohesive DSR	Improvement
Simulation			
\bar{f} (N)	0.146	0.014	90%
\bar{D} (cm)	5.824	0.563	90%
Experiment			
\bar{f} ($\mu \pm \sigma$) (N)	0.165 \pm 0.008	0.021 \pm 0.004	87 \pm 0.50%
\bar{D} ($\mu \pm \sigma$) (cm)	6.530 \pm 0.010	0.940 \pm 0.010	85 \pm 0.05%

TABLE I: Improvement (reduction) in maximum force (\bar{f}) and maximum deformation (\bar{D}) with cohesive DSR when compared to case without DSR. Top: Simulation results. Bottom: Experimental results with mean μ and standard deviation σ over 7 trials.

VI. CONCLUSION

An approach was presented to reduce deformation of objects during transport with decentralized robot networks. The approach used only local force measurements without additional communication, and conditions for stability were established. The proposed cohesive DSR approach was evaluated using simulation and the results closely matched the experimental results. Overall, the proposed approach led to 85% reduction in the deformation of the experimental system without increasing the time to transport the object to a new position. Ongoing efforts are focused on extending the approach to systems with high-order dynamics.

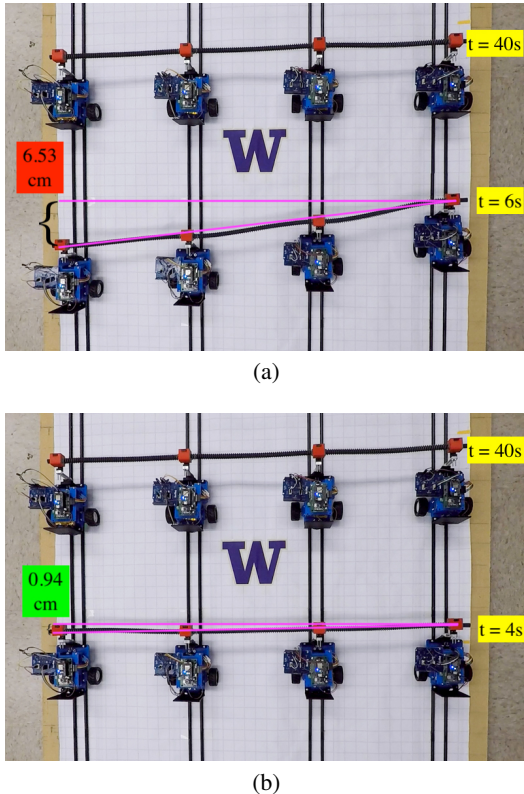


Fig. 7: Reduction in maximum deformation \bar{D} with cohesive DSR approach (at time $t = 4$ s) compared to the case without DSR (at time $t = 6$ s) as seen in video snapshots of the experiment overlaid with the positions at time $t = 40$ s: (top) without DSR, and (bottom) with cohesive DSR. The deformations over time are shown in Fig. 5f. Video of the experiment can be seen here: <https://youtu.be/tzDfnMbgIgA>.

REFERENCES

- [1] Y. E. Nesterov, "A Method of Solving a Convex Programming Problem with Convergence Rate of $O(1/k^2)$," *Soviet Mathematics Doklady*, vol. 27, no. 3, pp. 372–376, 1983.
- [2] B. Van Scoy, R. A. Freeman, and K. M. Lynch, "The fastest known globally convergent first-order method for minimizing strongly convex functions," *IEEE Control Systems Letters*, vol. 2, no. 1, pp. 49–54, Jan 2018.
- [3] Kar-Han Tan and M. A. Lewis, "Virtual structures for high-precision cooperative mobile robotic control," in *Proceedings of IEEE/RSJ International Conference on Intelligent Robots and Systems. IROS '96*, vol. 1, Nov 1996, pp. 132–139 vol.1.
- [4] B. Khoshnevis and G. Bekey, "Centralized sensing and control of multiple mobile robots," *Computers and Industrial Engineering*, vol. 35, no. 3, pp. 503 – 506, 1998, selected Papers from the 22nd ICC and IE Conference. [Online]. Available: <http://www.sciencedirect.com/science/article/pii/S0360835298001442>
- [5] A. Petitti, A. Franchi, D. Di Paola, and A. Rizzo, "Decentralized motion control for cooperative manipulation with a team of networked mobile manipulators," in *2016 IEEE International Conference on Robotics and Automation (ICRA)*, May 2016, pp. 441–446.
- [6] A. Tsiamis, C. K. Verginis, C. P. Bechlioulis, and K. J. Kyriakopoulos, "Cooperative manipulation exploiting only implicit communication," in *2015 IEEE/RSJ International Conference on Intelligent Robots and Systems (IROS)*, Sep. 2015, pp. 864–869.
- [7] Z. Wang and M. Schwager, "Kinematic multi-robot manipulation with no communication using force feedback," in *2016 IEEE International Conference on Robotics and Automation (ICRA)*, May 2016, pp. 427–432.
- [8] B. E. Jackson, T. A. Howell, K. Shah, M. Schwager, and Z. Manchester, "Scalable Cooperative Transport of Cable-Suspended Loads With UAVs Using Distributed Trajectory Optimization," *IEEE Robot. Autom. Lett.*, vol. 5, no. 2, pp. 3368–3374, Apr. 2020. [Online]. Available: <https://ieeexplore.ieee.org/document/9007450/>
- [9] Jianing Chen, M. Gauci, Wei Li, A. Kolling, and R. Gros, "Occlusion-Based Cooperative Transport with a Swarm of Miniature Mobile Robots," *IEEE Trans. Robot.*, vol. 31, no. 2, pp. 307–321, Apr. 2015. [Online]. Available: <http://ieeexplore.ieee.org/document/7055285/>
- [10] G. Montemayor and J. T. Wen, "Decentralized collaborative load transport by multiple robots," in *Proceedings of the 2005 IEEE International Conference on Robotics and Automation*, April 2005, pp. 372–377.
- [11] A. Gelblum, I. Pinkoviezky, E. Fonio, A. Ghosh, N. Gov, and O. Feinerman, "Ant groups optimally amplify the effect of transiently informed individuals," *Nature Communications*, vol. 6, no. 1, p. 7729, 2015. [Online]. Available: <https://doi.org/10.1038/ncomms8729>
- [12] H. Bai and J. T. Wen, "Cooperative load transport: A formation-control perspective," *IEEE Transactions on Robotics*, vol. 26, no. 4, pp. 742–750, Aug 2010.
- [13] G. Loianno and V. Kumar, "Cooperative Transportation Using Small Quadrotors Using Monocular Vision and Inertial Sensing," *IEEE Robot. Autom. Lett.*, vol. 3, no. 2, pp. 680–687, Apr. 2018. [Online]. Available: <http://ieeexplore.ieee.org/document/8120115/>
- [14] S. Thapa, R. V. Self, R. Kamalapurkar, and H. Bai, "Cooperative manipulation of an unknown payload with concurrent mass and drag force estimation," *IEEE Control Systems Letters*, vol. 3, no. 4, pp. 907–912, Oct 2019.
- [15] J. Alonso-Mora, R. Knepper, R. Siegwart, and D. Rus, "Local motion planning for collaborative multi-robot manipulation of deformable objects," in *2015 IEEE International Conference on Robotics and Automation (ICRA)*, May 2015, pp. 5495–5502.
- [16] S. Flixeder, T. Glück, and A. Kugi, "Modeling and Force Control for the Collaborative Manipulation of Deformable Strip-Like Materials," *IFAC-PapersOnLine*, vol. 49, no. 21, pp. 95–102, 2016. [Online]. Available: <https://linkinghub.elsevier.com/retrieve/pii/S2405896316321085>
- [17] E. Rossi, M. Tognon, R. Carli, L. Schenato, J. Cortes, and A. Franchi, "Cooperative Aerial Load Transportation via Sampled Communication," *IEEE Control Syst. Lett.*, vol. 4, no. 2, pp. 277–282, Apr. 2020.
- [18] S. Devasia, "Cohesive networks using delayed self reinforcement," *Automatica*, vol. 112, p. 108699, 2020. [Online]. Available: <http://www.sciencedirect.com/science/article/pii/S000510981930562X>
- [19] R. Olfati-Saber, J. Fax, and R. Murray, "Consensus and cooperation in networked multi-agent systems," *Proceedings of the IEEE*, vol. 95, no. 1, pp. 215–233, Jan 2007.